

Analytical approach calculating eigenfrequencies and modes of stator cores in AC machines*

PAWEŁ WITCZAK

*Institute of Mechatronics and Information Systems
 Technical University of Łódź
 Stefanowskiego 18/22, 90-924 Łódź
 e-mail: pawel.witczak@p.lodz.pl*

(Received: 11.12.2011, revised: 11.01.2012)

Abstract: The paper describes analytical approach solving the problem of dynamic analysis of two-dimensional fields of vibrational displacements and rotations caused by magnetic forces acting on stator of AC machine. Final set of three differential equations converted into algebraic ones is given and it is confronted with numerical solutions obtained by finite element method.

Key words: natural vibration, AC machines, differential equations

1. Introduction

The question of magnetic vibration in AC machines becomes a quite frequent topic of investigations. The method commonly used is the finite element (FE) technique enabling accurate analysis of free and forced vibration [2, 9, 10]. The geometry of stator core together with its composite material structure is the reason of fact that FE mesh discretising the volume of stator core and windings contains the definite majority of all elements used in the overall model of the motor. That problem is particularly troublesome in the case of large machines, when the number of slots may exceed one hundred. Another difficulty arises, related to the solution time of the numerical model, when the vibration analysis should be directly incorporated into optimization routine. Even ten minutes or so necessary to solve the small FE model are too much if it is repeated few hundred times. Therefore, investigation of fast and accurate method of vibration modeling seems still to be the important engineering subject in the domain of electric machines.

* This is extended version of a paper which was presented at the 47th International Symposium on Electrical Machines SME 2011, Szczecin, Poland.

2. Mechanical model of smooth ring

2.1. Plane displacements

Thick ring is the natural model of laminated stator core. Its dynamic behaviour under sinusoidal in space and time excitation is well known [1, 7] – the equation describing its natural angular frequencies of n -th order is

$$\left(\frac{\omega_n}{\omega_0}\right)^2 = \beta \frac{n^2(n^2 - 1)^2}{(n^2 + 1)}, \quad (1)$$

where $\beta = h^2/12R^2$ - h is ring thickness and R denotes its mean radius, see Figure 1. The normalisation constant ω_0 is so-called ring frequency (breathing mode), when ring surface moves uniformly up and down in radial direction only. The value of this constant is given by

$$\omega_0^2 = \frac{E}{R^2 \rho}, \quad (2)$$

where E is Young modulus and ρ is mass density. Such a model was the starting point for so-called “energy methods” [3, 4].

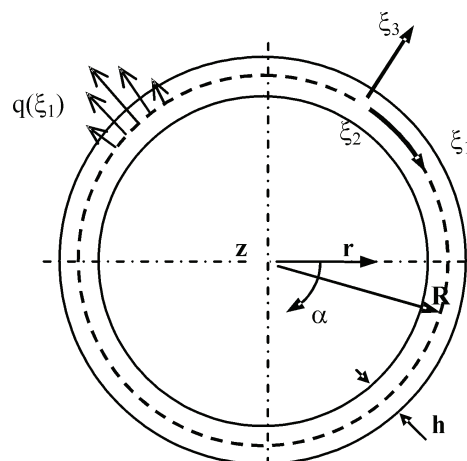


Fig. 1. Geometry of ring modeling the stator lamination

Fundamental assumption of above model is sufficiently smaller ring thickness h than its mean radius R . Apart from global cylindrical system of coordinates $r\alpha z$, a local one $\xi_1 \xi_2 \xi_3$ is also considered. Assuming that thickness h remains unchanged when ring is deformed, one may introduce two functions of unknown magnitudes describing displacements of mean ring surface (with $r = R$) along angle α in radial u_{30} and tangential u_{10} directions. If supporting system consists of virtual medium having very low stiffness and density these functions may be foreseen as

$$u_{10}(\alpha, t) = U_1 \sin(n\alpha) e^{j\omega t}, \\ u_{30}(\alpha, t) = U_3 \cos(n\alpha) e^{j\omega t}. \quad (3)$$

Exciting forces of linear densities $q_1(\alpha)$ and $q_3(\alpha)$ have zero mean value along circumference. A classic, quite sophisticated analysis leads [1, 7] to two differential equations

$$EI \frac{1}{R^4} \left(\frac{\partial^2 u_{10}}{\partial \alpha^2} - \frac{\partial^3 u_{30}}{\partial \alpha^3} \right) + E \frac{hg}{R^2} \left(\frac{\partial^2 u_{10}}{\partial \alpha^2} + \frac{\partial u_{30}}{\partial \alpha} \right) = -q_1 + \rho g h \frac{\partial^2 u_{10}}{\partial t^2}, \quad (4)$$

$$EI \frac{1}{R^4} \left(\frac{\partial^3 u_{10}}{\partial \alpha^3} - \frac{\partial^4 u_{30}}{\partial \alpha^4} \right) + E \frac{hg}{R^2} \left(\frac{\partial u_{10}}{\partial \alpha} + u_{30} \right) = -q_3 + \rho g h \frac{\partial^2 u_{10}}{\partial t^2}, \quad (5)$$

where I is the moment of inertia of rectangular cross-section

$$I = \frac{g h^3}{12} \quad (6)$$

and g is ring size along z axis. Introducing (3) into (4) and (5) one gets magnitudes U_1 , U_3 and also with $q_1 = q_3 = 0$ the set of natural frequencies ω_n shown earlier in equation (1). Application of above equations to the problem of vibration of stator core is usually done by simple increase of ring density representing in that way the presence of stator teeth and windings. Unfortunately, such a treatment may bring a considerable error for machines having long teeth. Therefore, some modifications inside the model are necessary.

2.2. Plane displacements and rotation

Bending is dominating type of deformation of ring geometry under forces of order $n > 0$. It means that radial component of displacement distribution along mean (neutral) surface has both positive and negative values. Simultaneously, neutral surface remains almost stress free. It results that line $Q_1 Q_2$ belonging to that surface and containing the point P_0 of zero displacement preserves its length and is rotated only against this point, what is displayed in Figure 2.

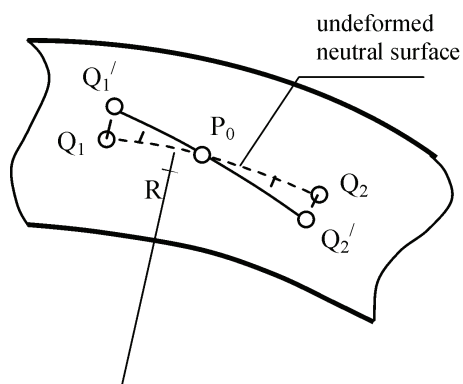


Fig. 2. Explanation of rotation in bended ring

The effect described is linked with additional inertia related to angular acceleration not included in previous model. It is possible to extend the set of unknown functions adding to equation (3) the distribution of angular displacement γ .

$$\begin{aligned}\gamma(\alpha, t) &= \Gamma \sin(n\alpha) e^{j\omega t}, \\ u_{10}(\alpha, t) &= U_1 \sin(n\alpha) e^{j\omega t}, \\ u_{30}(\alpha, t) &= U_3 \cos(n\alpha) e^{j\omega t}.\end{aligned}\quad (7)$$

Now three equations of motion are required for solution. They are obtained from infinitely small section of the ring being loaded by two-component force density applied to neutral surface. The distribution of force and torque components applied to infinitely small angular piece of ring $\delta\alpha$ are presented in Figure 3 [8].

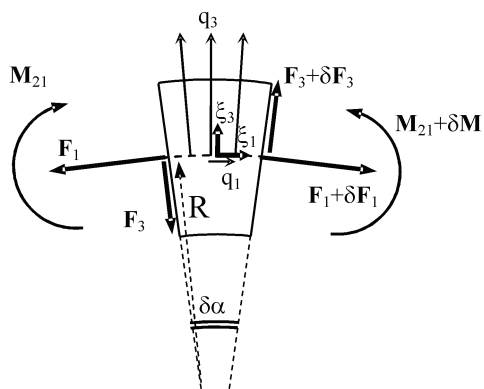


Fig. 3. Geometry of ring section for equilibrium analysis

The strain caused by local rotation can be represented within theory of infinitesimal displacements by means of shear strain ϵ_{13} , which is given by

$$\epsilon_{13} = \frac{1}{2} \left(\frac{\partial u_{10}}{\partial \xi_3} - \frac{u_{10}}{R} + \frac{\partial u_{30}}{\partial \xi_1} \right), \quad (8)$$

where factor u_{10}/R includes reduction of radial shift by tangent displacement due to ring curvature. Angle of rotation γ (between surfaces plotted in Fig. 2) may be represented by one of derivatives in (8) – they are in fact almost equal, but with opposite signs. Multiplying by shear stiffness $2G$ and integrating over surface one gets the tangent force F_3

$$F_3 = \kappa h g G \left(\gamma - \frac{u_{10}}{R} + \frac{\partial u_{30}}{R \partial \alpha} \right), \quad (9)$$

The coefficient κ equals to $5/6$, after Timoshenko theory [8].

The angular motion equation will be

$$+ \frac{\partial M_{21}}{\partial \alpha} - F_3 R = \rho I \frac{\partial^2 \gamma}{\partial t^2} R. \quad (10)$$

Bending torque can be expressed [8] as

$$M_{21} = EI \frac{1}{R^2} \left(\frac{\partial u_{10}}{\partial \alpha} - \frac{\partial^2 u_{30}}{\partial \alpha^2} \right), \quad (11)$$

what finally gives

$$EI \frac{1}{R^2} \left(\frac{\partial^2 u_{10}}{R \partial \alpha^2} - \frac{\partial^3 u_{30}}{R \partial \alpha^3} \right) + \kappa h g G \left(\gamma - \frac{u_{10}}{R} + \frac{\partial u_{30}}{R \partial \alpha} \right) = \rho I \frac{\partial^2 \gamma}{\partial t^2}. \quad (12)$$

We cannot use directly Equations (4)(5) as missing supplements for (12), because they were derived under assumption $\varepsilon_{13} = 0$ giving another than (9) expression for F_3 . The equilibrium equations for movements along ξ_1 and ξ_2 have general form

$$\begin{aligned} \frac{F_3}{R} + \frac{\partial F_1}{R \partial \alpha} &= -q_1 + \rho g h \frac{\partial^2 u_1}{\partial t^2}, \\ -\frac{F_1}{R} + \frac{\partial F_3}{R \partial \alpha} &= -q_3 + \rho g h \frac{\partial^2 u_3}{\partial t^2}. \end{aligned} \quad (13)$$

Additions F_1/R and F_3/R arise from ring curvature. In order to get relation describing F_1 we have to know membrane strain component along neutral layer – bending strain does not contribute to that force. Following strain definition we have

$$F_1 = Ehg \left(\frac{1}{R} \frac{\partial u_{10}}{\partial \alpha} + \frac{u_{30}}{R} \right). \quad (14)$$

Substituting relations (9) and (14) into (13) we have

$$\frac{hg}{R} \kappa G \left(\gamma - \frac{u_{10}}{R} + \frac{\partial u_{30}}{R \partial \alpha} \right) + \frac{hg}{R} E \left(\frac{1}{R} \frac{\partial^2 u_{10}}{\partial \alpha^2} + \frac{\partial u_{30}}{R \partial \alpha} \right) = -q_1 + \rho g h \frac{\partial^2 u_{10}}{\partial t^2}, \quad (15)$$

$$\frac{hg}{R} \kappa G \left(\frac{\partial \gamma}{\partial \alpha} - \frac{\partial u_{10}}{R \partial \alpha} + \frac{\partial^2 u_{30}}{R \partial \alpha^2} \right) - \frac{hg}{R} E \left(\frac{\partial u_{10}}{R \partial \alpha} + \frac{u_{30}}{R} \right) = -q_3 + \rho g h \frac{\partial^2 u_{30}}{\partial t^2}. \quad (16)$$

The next step it is to find magnitudes of investigated functions (7). Inserting these relationships into (12) (15) (16), after few manipulations one may obtain the following set of equations, which is written in the classic form suitable both for forced and free vibration analysis

$$([\mathbf{A}] - \omega^2 [\mathbf{I}]) \begin{Bmatrix} \Gamma \\ U_3 \\ \frac{R}{U_3} \\ \frac{U_1}{R} \end{Bmatrix} = \begin{Bmatrix} 0 \\ q_3 \\ \frac{\rho g h R}{\Gamma} \\ \frac{q_1}{\rho g h R} \end{Bmatrix}, \quad (17)$$

where $[\mathbf{I}]$ is identity matrix and $[\mathbf{A}]$ matrix amounts to

$$[\mathbf{A}] = \begin{bmatrix} \omega_{GI}^2 & n(\omega_{GI}^2 - \omega_0^2 n^2) & \omega_0^2 n^2 + \omega_{GI}^2 \\ -n\omega_G^2 & \omega_G^2 n^2 + \omega_0^2 & n(\omega_G^2 + \omega_0^2) \\ -\omega_G^2 & n(\omega_G^2 + \omega_0^2) & \omega_G^2 + n^2 \omega_0^2 \end{bmatrix}. \quad (18)$$

Particular constants denote

$$\begin{aligned} \omega_{GI}^2 &= \frac{\kappa g h}{\rho I} G, \\ \omega_G^2 &= \frac{\kappa}{\rho R^2} G, \\ \omega_0^2 &= \frac{1}{\rho R^2} E. \end{aligned} \quad (19)$$

Further simplifications are possible dividing both sides of (17) by ω_0^2 . For isotropic continuum the modules E and G are directly proportional through $2(1+\nu)$. Setting Poisson coefficient ν to 0.3 we have

$$\begin{aligned} \left(\frac{\omega_G}{\omega_0}\right)^2 &= \frac{\kappa}{2(1+\nu)} = i_G \cong 0.32, \\ \left(\frac{\omega_{GI}}{\omega_0}\right)^2 &= \frac{12\kappa}{2(1+\nu)} \left(\frac{R}{h}\right)^2 = i_{GI} \cong 3.84 \left(\frac{R}{h}\right)^2. \end{aligned} \quad (20)$$

Equations (17) are converted to

$$\left([\mathbf{A}_0] - \left(\frac{\omega}{\omega_0}\right)^2 [\mathbf{I}]\right) \begin{Bmatrix} \Gamma \\ U_3 \\ \frac{R}{U_1} \\ \frac{R}{R} \end{Bmatrix} = \frac{1}{\omega_0^2} \begin{Bmatrix} 0 \\ q_3 \\ \frac{q_3}{\rho g h R} \\ \frac{q_1}{\rho g h R} \end{Bmatrix} \quad (21)$$

and matrix $[\mathbf{A}_0]$ amounts to

$$[\mathbf{A}_0] = \begin{bmatrix} i_{GI} & n(n^2 - i_{GI}) & n^2 - i_{GI} \\ -ni_G & n^2 i_G + 1 & n(i_G + 1) \\ -i_G & n(i_G + 1) & i_G + n^2 \end{bmatrix}. \quad (22)$$

Coefficients of $[\mathbf{A}_0]$ depend on dimensionless values of mode order n and ratio $(R/h)^2$ only. Comparing results obtained by the above approach with previously described method using displacements only, we will get very similar results, therefore, introduction of rotation is not mandatory while the smooth ring is analysed. On other hand, the presence of rotation in description of ring motion enables the further development of this model towards proper representation of slotted structure.

3. Mechanical model of stator lamination

Geometry of lamination sheet of typical multipole AC motor – in example given below $2p = 8$, is presented in Figure 4. It is assumed that no constraints exist in surrounding medium and also external forces of electromagnetic nature belonging to $\mathbf{r}\alpha$ plane are balanced in space and time.

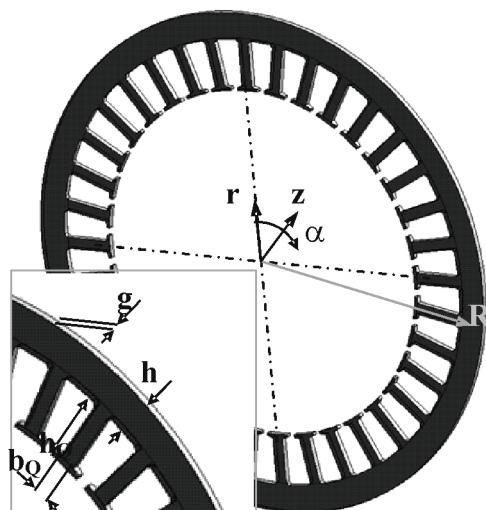


Fig. 4. Geometry of single lamination sheet of AC motor

The key assumption in modeling the behaviour of stator teeth is that they follow local yoke displacements and rotation in form of rigid body motion. It means that presence of teeth on one side of the ring changes its inertial properties only. The inertial term in Equations (15) (16) is related to displacements, therefore, mass density must be increased by the ratio k_ρ of lamination to yoke mass,

$$k_\rho = 1 + \frac{Qb_Q h_Q}{2\pi Rh} , \quad (23)$$

where Q is number of teeth and remaining dimensions are displayed in Figure 4. The modification of Equation (12) is a bit more complicated. We want to account the increase of angular inertia of continuous ring structure, which was induced by the discrete set of teeth. It will be done in few steps. Firstly, the real shape of single tooth is reduced to the rectangle as it is shown in Figure 5.

The main moment of inertia of the cuboid against axis passing through its gravity center is

$$J_{z0} = \rho I_{z0} \left(1 + \left(\frac{b_Q}{h_Q} \right)^2 \right) b_Q , \quad (24)$$

where I_{z0} is moment of inertia of the rectangle (h_Q, g) against its symmetry axis along side g . Tooth is rotated about axis z_n situated on neutral layer, so, after Steiner theorem, the moment of tooth inertia about z_n equals to

$$J_{zn} = J_{z0} + m_Q d^2, \quad (25)$$

where m_Q is tooth mass. After few manipulations we may have

$$J_{zn} = \rho I_{z0} \left[1 + \left(\frac{b_Q}{h_Q} \right)^2 + 3 \left(1 + \frac{h}{h_Q} \right)^2 \right] b_Q. \quad (26)$$

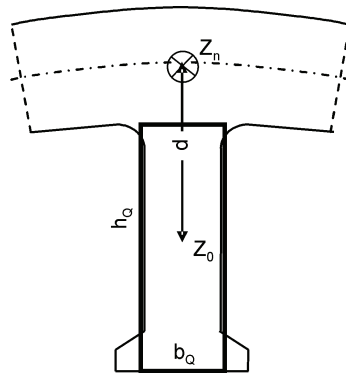


Fig. 5. Simplified geometry of lamination tooth

The ring equation (12) requires continuous properties like linear force density, therefore, we must “spread” the tooth inertia J_{zn} along the slot pitch measured on neutral layer. It may be now added to moment of inertia of yoke cross-section (6). It will be done by means of multiplication factor k_I increasing the value of I .

$$k_I = 1 + \left(\frac{h_Q}{h} \right)^3 \left[1 + \left(\frac{b_Q}{h_Q} \right)^2 + 3 \left(1 + \frac{h}{h_Q} \right)^2 \right] \frac{Q b_Q}{2\pi R}. \quad (27)$$

The change of overall mass also influences the value of reference angular frequency ω_0

$$\omega_{0z}^2 = \frac{\omega_0^2}{\kappa_\rho}. \quad (28)$$

Finally, substituting all additions (23) (27) (28) related to the presence of slots and simplifying the forcing term on the right side it is possible to write the set of equations (21) in form

$$\left([\mathbf{A}_{0z}] - \left(\frac{\omega}{\omega_{0z}} \right)^2 [\mathbf{I}] \right) \begin{Bmatrix} \frac{\Gamma}{U_3} \\ \frac{R}{U_1} \\ \frac{R}{U_1} \end{Bmatrix} = \frac{R}{Egh} \begin{Bmatrix} 0 \\ q_3 \\ q_1 \end{Bmatrix} \quad (29)$$

and corrected matrix $[\mathbf{A}_{0z}]$ is given by

$$[\mathbf{A}_{0z}] = \begin{bmatrix} \frac{k_\rho}{k_I} i_{GI} & n \frac{k_\rho}{k_I} (n^2 - i_{GI}) & \frac{k_\rho}{k_I} (n^2 - i_{GI}) \\ -ni_G & n^2 i_G + 1 & n(i_G + 1) \\ -i_G & n(i_G + 1) & i_G + n^2 \end{bmatrix}. \quad (30)$$

Solving the eigenvalue problem for exemplary lamination in two ways – analytical, based on Equations (29), (30) and numerical by FE approach, the results obtained are confronted in Table 1.

Table 1. Comparison of analytic and numeric solutions of relative natural frequencies obtained for sheet given by: $n_z = 36$, $R = 0.08$ m, $h = 0.01$ m, $h_z = 0.018$ m, $b_z = 0.004$ m, $k_\rho = 1.49$, $k_I = 14.2$

Method	Relative natural frequency ω_n/ω_{0z}				Ring frequency [rad/s]
	$n = 2$	$n = 3$	$n = 4$	$n = 5$	
Analytic, Eq. (1)	0.093	0.261	0.501	0.810	49.2
Analytic, Eq. (29)	0.091	0.252	0.467	0.728	49.2
Numeric	0.091	0.245	0.441	0.642	48.6

The agreement obtained for modes of the lowest order is very good, for higher modes a few percent discrepancy has appeared. It can be explained observing the shapes of investigated modes visualised by FE software in Figure 6. Looking on lowest mode of order $n = 2$ we see that all teeth are perpendicular to deflected mean line of yoke fulfilling in that way the assumption of purely inertial nature of vibrational behaviour of teeth. But in the case of higher order $n = 5$ one can see bended outline of most of teeth. It means stator teeth do not behave like rigid body as it was assumed initially. That influence on values of calculated natural frequencies is not very substantial but visible. This effect is a natural limit of presented method.

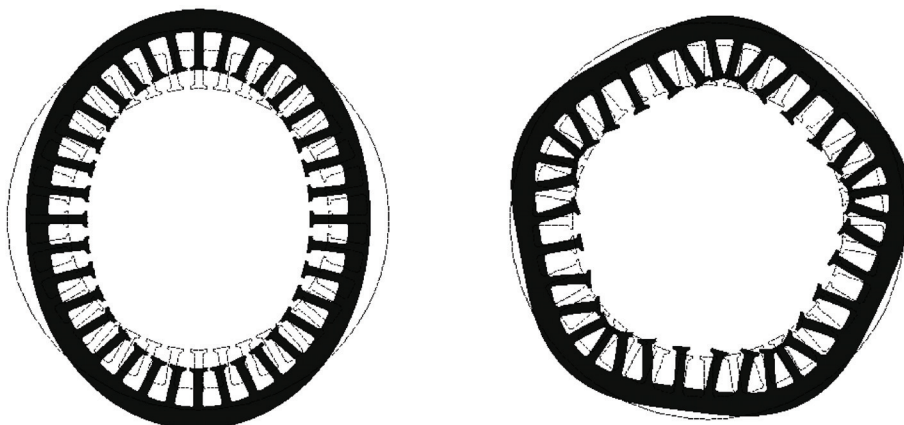


Fig. 6. Shapes of natural modes of order $n = 2$ and $n = 5$

4. Conclusions

The calculation method described in the paper enables fast and accurate estimation of natural frequencies for modes of lowest order. It means that it can be also applied for forced vibration in a quite wide range of exciting frequencies. Its accuracy near resonances will not be very good because of absence of components representing the energy dissipation in equations of motion. They may be added in a standard way [5, 6] converting solution into complex domain. The another application foreseen in a future work is the search of equivalent anisotropic ring structure for slotted lamination. Such a problem cannot be solved explicitly because of its nonlinear relationships – it requires iterative approach, where a computation time is one of decisive factors when the method of modeling is chosen.

The paper was done within the project N510 590440 granted by Ministry of Science and Higher Education, Republic of Poland.

References

- [1] Cremer L., Heckl M., Petersson B.A.T., *Structure-borne sound*, Springer Verlag, Berlin (2005).
- [2] Delaere K. *Computational and experimental analysis of electric machine vibrations caused by magnetic forces and magnetostriction*, PhD Thesis, Katholieke Universiteit Leuven (2003).
- [3] Ellison A.J., Yang S.J., *Natural frequencies of stators of small electric machines*. Proceedings of the IEE, 118(1): 185-190 (1971).
- [4] Girgis R.S., Verma S.P., *Method for accurate determination of resonant frequencies and vibration behaviour of stators of electrical machines*. Electric Power Applications, IEE Proceedings B, 128(1): 1-11 (1981).
- [5] Norton M., Karczub D., *Fundamental of noise and vibration analysis for engineers*, Cambridge University Press (2003).
- [6] Rao S.S., *Vibration of continuous systems*, John Wiley & Sons Inc. (2007).
- [7] Soedel W., *Vibration of shells and plates*, Marcel Dekker Inc. (2004).
- [8] Timoszenko S., Goodier J.N., *Teoria sprężystości*, Arkady, Warszawa (1962).
- [9] Wang H., Williams K., *The vibrational analysis and experimental verification of a plane electrical machine stator model*. Mechanical Systems and Signal Processing 9(4): 429-438 (1995).
- [10] Witczak P., *Wyznaczanie drgań mechanicznych w silnikach indukcyjnych wywołanych silami magnetycznymi*, Zesz. Nauk. Politechniki Łódzkiej 725 (1995).